



Cite this: DOI: 10.1039/c8lc00228b

Received 5th March 2018,
Accepted 8th May 2018

DOI: 10.1039/c8lc00228b

rsc.li/loc

Large-scale patterning of living colloids for dynamic studies of neutrophil–microbe interactions†

Jae Jung Kim,^{†a} Eduardo Reátegui,^{‡§bc} Alex Hopke,^b Fatemeh Jalali,^b Maedeh Roushan,^b Patrick S. Doyle^{†*a} and Daniel Irimia^{†*b}

Neutrophils are the first white blood cells to respond to microbes and to limit their invasion of the body. However, the growth of the microbes into colonies often challenges the neutrophils ability to contain them. To study the interactions between neutrophils and microbial colonies, we designed an assay for arranging microbes in clusters of controlled size (*i.e. living colloids*). The patterned microbes in the living colloid are mechanically trapped inside the wells and fully accessible to neutrophils. Using the assay, we studied the interactions between human neutrophils and *Candida albicans* and *Staphylococcus aureus*, two common human pathogens. We also probed the susceptibility of *C. albicans* colloids to caspofungin, a common antifungal drug.

The study of microorganisms and interactions with the immune system has long been centered on pure populations in a planktonic state. While these studies have generated a wealth of knowledge, it is now appreciated that microbes are rarely found in isolation. Instead, most often they live in complex communities on and inside the body.^{1–4} The composition, interactions, and evolution over time of the microbial communities is of clinical importance.^{4–12} Despite advances in understanding microbial communities in infections, much is still unknown. Studying microbial communities' behaviour and interactions with the host in a rapid, high throughput manner would be highly beneficial. However, such studies have been challenging to pursue, due

in part to a lack of adequate tools. “Patterning” of microorganisms, where one controls the spatial arrangement of microbes, has emerged as a promising technique to study microbial populations. For example, one of the promising approaches is the positioning of microorganisms in single layers on adherent surfaces.^{13–17} Applications include the diagnostics,¹⁸ antibiotic susceptibility testing,^{19–21} genotoxic monitoring,²² high-throughput screening,^{23,24} and environmental monitoring.²⁵ They are also useful in fundamental studies of biological phenomena, including host–pathogen interactions,²⁶ horizontal gene transfer,²⁷ quorum sensing^{28,29} and biofilm assembly.^{30–32}

Passive settlement in micro-well arrays can also achieve large-scale cell patterning of cells at pre-defined locations.³³ However, this method is not suitable for patterning microorganisms because their small size (1–10 μm) results in long assembly time. Micro-well-based techniques have several advantages including control of geometric features, scalability, versatility, and precision. Several groups have therefore tried to overcome the low throughput of passive settlement by using centrifugal,^{22,23} surface tension,³⁴ and hydrodynamic forces.^{35,36} However, most approaches^{22,23,35} are focused on single cell arrays. The ability to generate densely-filled micro-organism patterns, which could be useful for the study of microbe communities, was not systematically explored. Both single-cell and densely-filled pattern were generated by surface tension-based cell docking.³⁴ However, the procedure takes 10–20 minutes, during which the small volume of solution in wells can dry, damaging the microbes.

It is desired to pattern microorganisms at a precise location in large-scale arrays with an ability to fine-tune the geometry of the patterns. The technique should also be versatile and adequate for patterning a variety of microorganisms. Achieving high-throughput with a short processing time is key for handling fast growing, live microbes. Unfortunately, all existing systems have limited control over the microorganisms in the array, while pre-patterned chemical layers can cause physiological changes in microorganisms. Thus, there

^a Department of Chemical Engineering, Massachusetts Institute of Technology, Cambridge, MA, 02139, USA. E-mail: pdoyle@mit.edu

^b BioMEMS Resource Center, Massachusetts General Hospital, Harvard Medical School, and Shriners Hospital for Children, MA, 02129, USA.

E-mail: dirimia@mgh.harvard.edu

^c Massachusetts General Hospital Cancer Center, Harvard Medical School, MA, 02129, USA

† Electronic supplementary information (ESI) available. See DOI: 10.1039/c8lc00228b

‡ These authors contributed equally to this work.

§ Current address: William G. Lowrie Department of Chemical and Biomolecular Engineering and Comprehensive Cancer Center, The Ohio State University, Columbus, OH, 43210, USA.

is a need for appropriate materials for each specific microorganism. Direct printing of microorganisms (*i.e.* an inkjet method) is a method that can directly pattern microbes without the need for chemical layers but it is limited to microbes that adhere directly to the glass and its resolution is limited to $\sim 100\ \mu\text{m}$.³⁷

Here, we demonstrate the use of porous micro-well arrays to generate large-scale living colloid arrays. A hydrodynamic force is driving the microorganisms inside patterns and enables the arrangement of fungi and bacteria with high precision in large scale arrays. Furthermore, the assembly template provides the ability to control the geometry of each microorganism cluster. With our platform, we patterned living fungi and bacteria. We explored the utility of these patterns as an *in vitro* testing system, conducting antibiotic susceptibility testing and interrogating host–pathogen interactions using fluorescence microscopy. We observed dose-dependent fungicidal activity in our system when testing the echinocandin caspofungin on *C. albicans*. During incubation with human cells, we observed and tracked directed neutrophil migration towards our microbial targets. We also analysed the supernatants and were able to detect numerous chemokines and cytokines relevant to inflammation.

We fabricated porous micro-wells on top of a polyethylene terephthalate (PET) membrane by a vacuum-assisted molding method inspired by a previous study³⁸ (Fig. 1, left. See the detail in the ESI†). Compared to the microstamping,³⁶ vacuum-assisted molding method provides higher resolution of patterning and more precise control in height. We fine-tuned the geometry and the spacing of micro-wells to control the microbe patterns. This platform can be fabricated with any photo/thermal curable materials (*e.g.*, polydimethylsiloxane (PDMS)). We selected NOA 81 in this study due to the fast curing time and biocompatibility.³⁹ To generate patterns, microorganism suspensions were dispensed on top of this platform, and negative pressure was applied to the bottom of the PET membrane. The applied pressure generates a fluid flow through the open pores in wells, and a hydrodynamic force associated with this flow guides the microorganism into micro-wells. This hydrodynamic force fulfills critical criteria of particle arrangement, enabling large-scale, high-throughput patterning: it has a controllable magnitude, converges into arrangement templates, and acts on any colloidal particles in the same manner regardless of their composition. As a result of microorganism guiding, this assembly process produces wells that are densely packed with

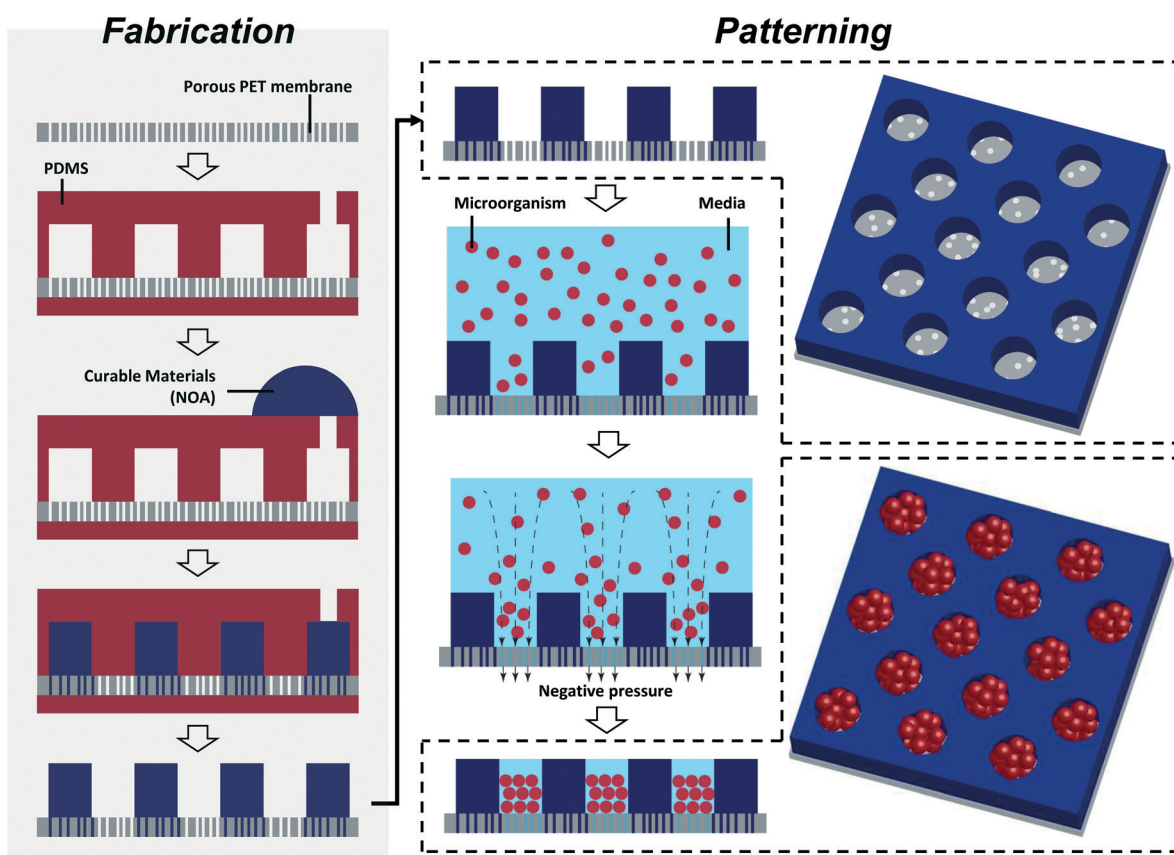


Fig. 1 Porous microwells for microorganism patterning in large arrays. NOA porous microwells are fabricated using vacuum-assisted molding method (left column, shaded). Flat and patterned PDMS blocks sandwich the porous PET membrane. Photo-curable NOA is injected to the mold using pressure difference generated by vacuum, and cured to obtain the porous microwells. To pattern microorganisms, a suspension of microorganisms was added on top of fabricated microwells, and hydrodynamic force guided microorganisms to microwells. After arrangement, redundant microorganisms were washed out to obtain patterned microorganisms.

microorganisms (Fig. 1, middle). Unlike the previous study,³⁸ where the size of microwells was closely matched with arranged objects, here we optimized the assay for dense packing of smaller microorganisms inside large arrays. The dense packing of microorganisms, combined with the depth of the micro-wells, shear-protect the microorganisms in the subsequent washing steps. Patterned microorganisms retained their position. Only redundant microorganisms (*i.e.*, ones outside wells) were removed when the platform was washed by flowing media across the top of the micro-wells (Fig. 1, bottom right). The patterned microorganisms are mechanically trapped in microwells and thus are fully accessible to neutrophils.

We patterned *C. albicans*, a clinically relevant fungus, to validate the new assay. Invasive fungal infections are a significant problem in the clinic and are associated with unacceptably high mortality rates.⁴⁰ *C. albicans* specifically can act as an opportunistic pathogen capable of causing both mucocutaneous and invasive disseminated disease, with invasive candidiasis estimated to have mortality up to 40%.⁴⁰ Here, we generated large-scale patterning of the yeast form *C. albicans* (Fig. 2a) into micro-wells ($D = 28 \mu\text{m}$ and $H = 35 \mu\text{m}$) which has much smaller dimension than the resolution of direct printing ($\sim 100 \mu\text{m}$). About 4000 patterns were generated within 2 iterations of guiding and washing, where each cycle takes approximately 30 seconds (Fig. 2b). The short processing time (60 s) and the ability to fabricate large numbers of micro-wells result in our platform's large-scale, high-throughput performance. The driving force and shear protection ensure high patterning yield. Typically, $93.5 (\pm 2.4)\%$ of micro-wells are filled. The relative standard deviation of pattern size was $26.0 (\pm 0.8)\%$. Demonstrating the flexibility of

our design, we were able to scale up the platform area to 1 cm^2 , corresponding to 32 000 micro-wells, with this limitation derived from the area of commercially available PET membrane. We confirmed, using confocal laser scanning microscopy (CLSM), that microorganisms were densely packed and filled ~ 60 (v/v)% of micro-well volume (Fig. 2b, Fig. S3†). The growth of *C. albicans* was monitored by time-lapse imaging (Movie S1†).

The ability of our platform to rapidly arrange microbes with large-scale, high-throughput performance enabled us to interrogate different aspects of *C. albicans* biology. Typically, techniques for fungal studies are relatively low throughput, often using a 96 well plate format or lower for detailed imaging and indirect methods (XTT/MTT reduction assay) to examine viability.^{41–43} Using our platform, we could also rapidly assess the susceptibility of *C. albicans* to different concentrations of antifungal drugs (Fig. 3a). We used a *C. albicans* strain with a constitutively expressed fluorescent protein in its cytoplasm. This fluorescence disappears following loss of cellular integrity and fungal death, which enables us to visually monitor the viability of *C. albicans*.^{44,45} Compared to an untreated control, caspofungin (Merck & Co., Inc.) decreased the growth rate and viability (as measured by fluorescent intensity) of *C. albicans* in a dose-dependent manner, with obvious fungicidal activity at 500 ng mL^{-1} (Fig. 3b). When grown alone, or in the presence of low doses of antibiotic, patterned *C. albicans* remains viable inside the microwells, grows, and forms hyphae radiating outwards from the microwells (Movie S2†). The radiating hyphae are likely responsible for the increase of the fluorescence outside the wells over time (Fig. 3a). By providing tight control over the size and locations of microbe clusters, our platform provides important

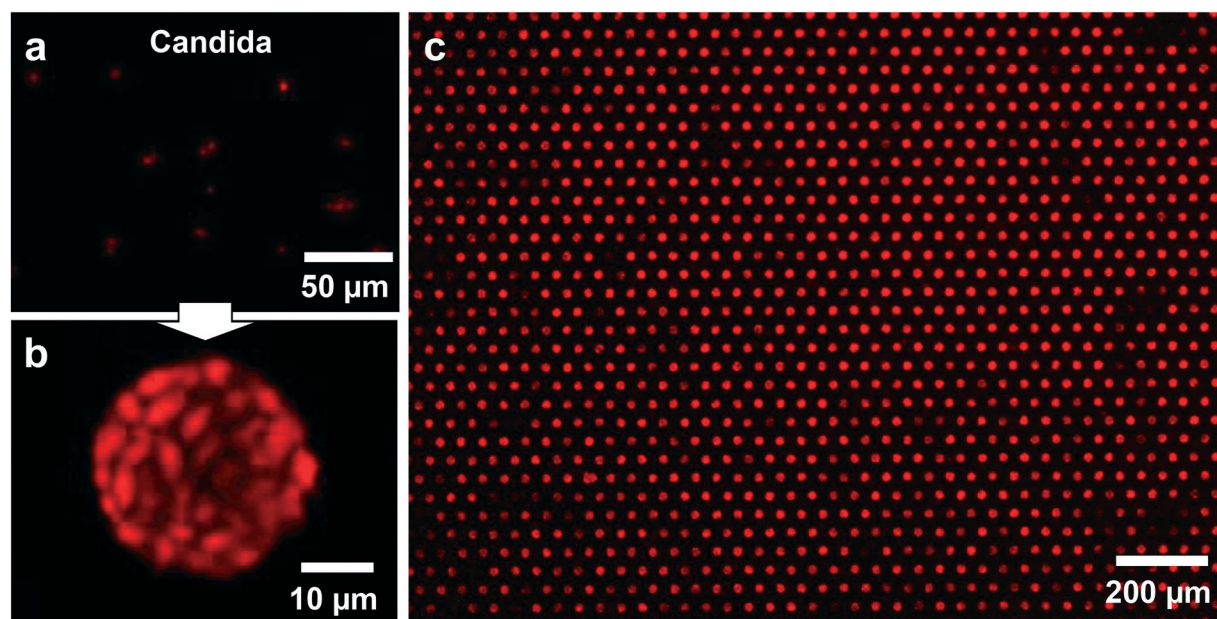


Fig. 2 Large-scale, high-throughput arrangement of *C. albicans* clusters. a) A suspension of planktonic *C. albicans* yeast. b) Densely packed *Candida* cells inside one porous microwell. Image is obtained using confocal microscopy. c) Large-scale *Candida* colloid arrays generated using porous microwell arrays. Typically, $93.5 (\pm 2.4)\%$ of the wells present *C. albicans*.

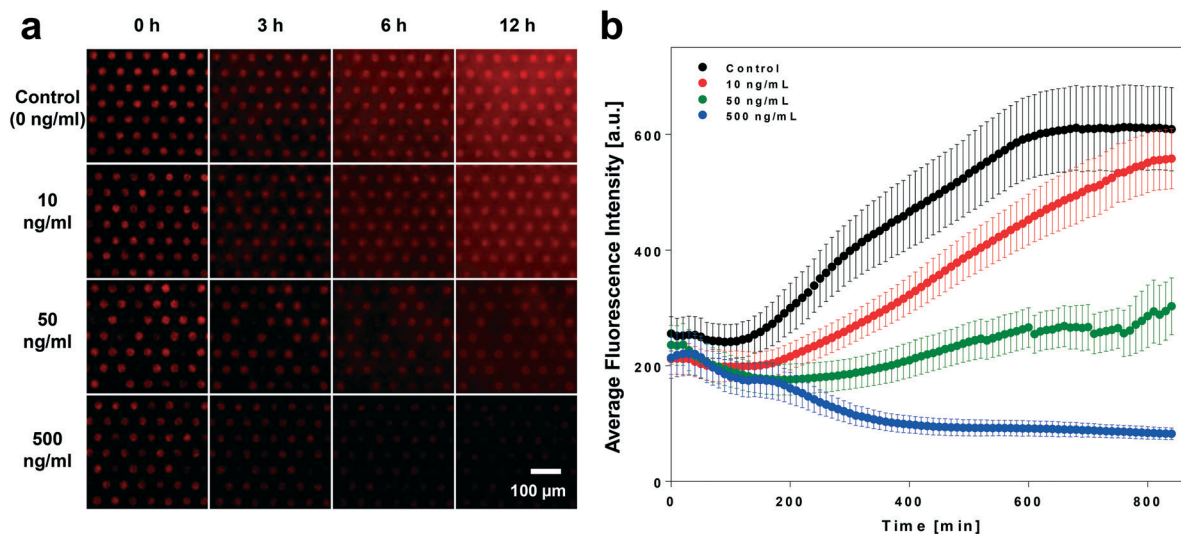


Fig. 3 Antifungal susceptibility testing with *C. albicans* and caspofungin. Patterned *C. albicans* are incubated with media containing different concentrations of caspofungin. a) Representative panels from time-lapse images showing the concentration dependent inhibition of growth. b) Plot showing *C. albicans* viability over the time. The fluorescent intensity indicates *C. albicans* viability. Error bar indicates the standard deviation of fluorescent intensity ($N = 36$).

advantages over traditional antifungal susceptibility testing like the micro-dilution, Etest, or XTT/MTT reduction assays. For research applications, it helps to directly visualize the responses of the fungi to immune cells and antibiotics. Furthermore, beyond a bulk readout of the average susceptibility in a fungal population, our platform allows the interrogation of any heterogeneity in fungal responses, as each microwell could also be followed individually during the assay.

Immune responses to infection and inflammation have been studied with *in vitro* and *in vivo* systems that interrogated the dynamics of these processes. Although these studies have improved our understanding of the immune response, *in vivo* systems^{46–48} have limited controllability of conditions and quantification of signalling molecules. Moreover, *in vivo* systems are frequently limited to animal models, potentially not identical to human.⁴⁹ Various *in vitro* systems, which utilize human leukocytes, have been tested using gradients of cytokines,^{38,50–52} fungi-wall mimicking particles,^{53,54} and living microorganisms.²⁶ However, these systems still lack the precision of patterning living microorganism while allowing for both chemotactic quantification and molecular analysis during immune response. A key advantage of our platform is that chemotactic and molecular quantification can be achieved. Once *C. albicans* were precisely patterned, we added isolated human neutrophils from fresh, healthy donor blood purchased from Research Blood Components (Allston, MA, USA). Due to the optical transparency of our platform, we could monitor the interactions between neutrophils and living microbial colloids by time-lapse fluorescent microscopy (Fig. 4a, Movie S3[†]). Our platform allowed us to precisely track individual neutrophils during migration (Fig. 4b) and to quantify different kinematic parameters. We found that most neutrophils migrate towards the target during the first eight minutes, followed by a plateau phase in which no more

cells are recruited (Fig. 4c). As the target strongly attracts the neutrophils, chemotactic index has a high value, close to 1 (see the ESI[†] for the calculation method). We observed that neutrophil migration is not random, as the calculated chemotactic index shows persistent positive values (Fig. 4d). Negative values would indicate non-chemotactic cells or cells migrating towards other targets in the array.

Once the first neutrophils engage with the pattern microorganisms, they release a cascade of chemokines and cytokines that amplify the process of immune cell recruitment, triggering a coordinated neutrophil migration towards each micro-well. This process is known as neutrophil swarming. Swarming has been reported *in vivo*,⁵⁵ but no microtechnologies have able to reproduce this complex cellular behaviour in the presence of live targets *in vitro*. Only one recent *in vitro* technology used patterned zymosan particles that mimicked fungi.⁵⁴ The platform presented in this manuscript offers an advantage over previous swarming microtechnologies, as we can easily use live microbial targets in swarming studies. The live targets are not attached to surfaces and can be picked up by neutrophils, avoiding the potential confounding effect of frustrated phagocytosis. Moreover, swarming studies have been used to develop comparative studies between healthy and diseased individuals, suggesting our platform can also be applied to study the biology of swarming during health and disease.⁵⁴

In addition to microscopic analysis, our platform facilitates access to secreted molecules during neutrophil microbe interactions (Fig. 4e). The volume of fluid on top of the array is small, enabling the rapid concentration of secreted molecules. This volume can be accessed directly with a standard pipette and collected for analysis. The array configuration assures that host–pathogen interactions are replicated in identical conditions multiple times, while the large size of the

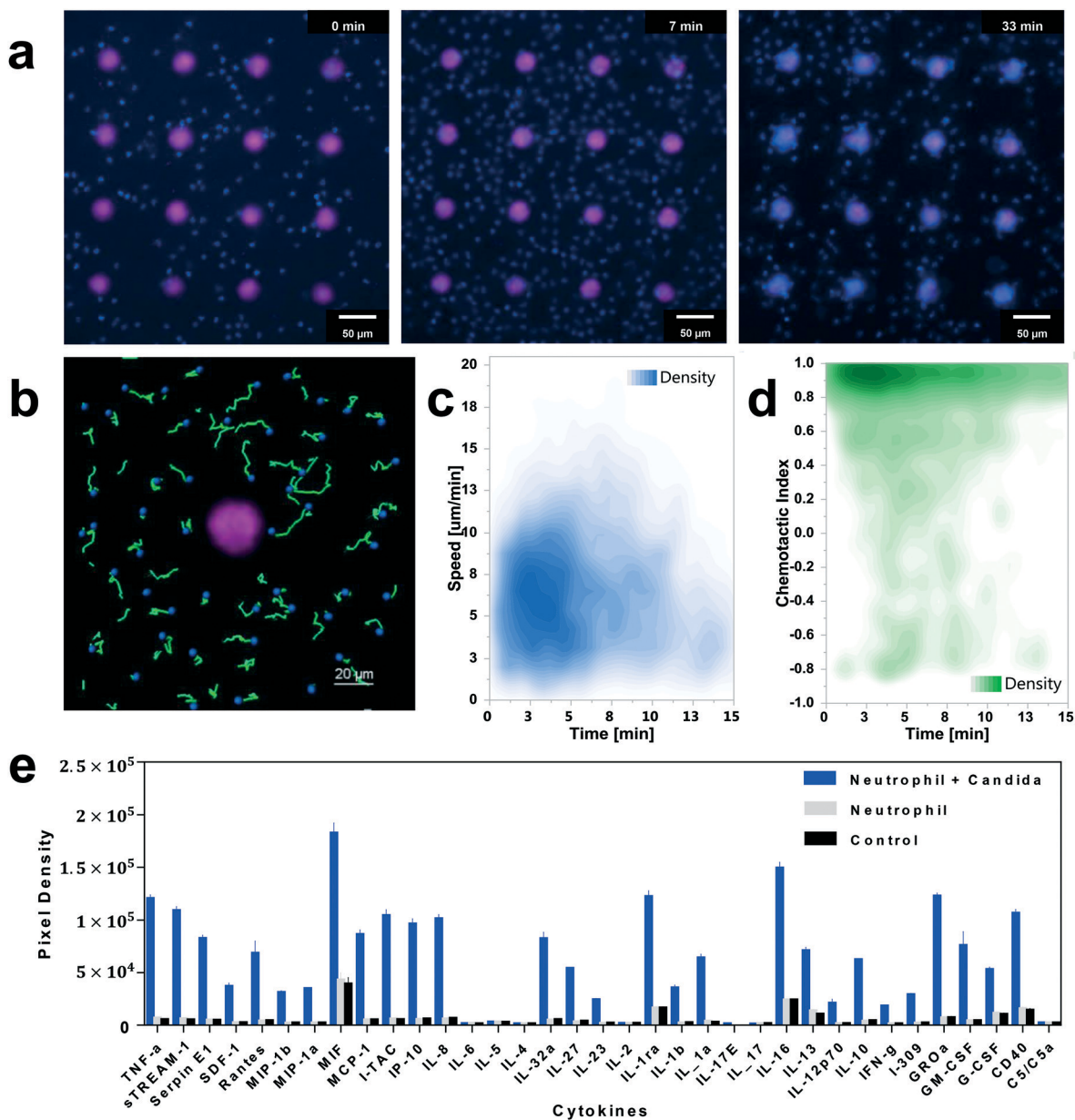


Fig. 4 The study of host–pathogen interactions between *C. albicans* and human neutrophils using porous microwells. Human neutrophils stained with Hoechst dye were loaded on the array and allowed to interact with *C. albicans*. **a**) Representative images from time-lapse microscopy. **b–d**) Microscopic analysis of human neutrophils' migration: Tracking result (**b**) and density plot of speed migration (**c**) and chemotactic index over the time (**d**). The plots are a characteristic representation of a single *C. albicans* pattern during neutrophil migration. **e**) Analysis of neutrophil migration at a molecular level. Supernatants were harvested following interaction between neutrophils and *C. albicans* arrays and analyzed by ELISA-based assay (Proteome Profiler Human Cytokine Array Kit, R&D systems). Higher pixel density of ELISA based assay indicates the existence of higher concentration of cytokines ($N = 3$). Two different controls were used: neutrophil media and media with suspended neutrophils (not *C. albicans*).

array assures a substantial increase the concentration of the secreted molecules in the supernatant. We examined the cytokines following the interaction of human neutrophils and patterned *C. albicans*. We identified molecules that mediate neutrophil, monocyte and lymphocyte recruitment (TNF- α , CCL5, CCL3, CCL4, CXCL8, IL-1a, CCL2, IL-23), neutrophil activation (sSTREAM-1). We also identified several cytokines that reduce inflammation (IL-10; IL13, IL-1ra). The levels of the cytokines tested were different from the two controls analysed: pure media; and media containing only neutrophils.

In addition to fungi, other bacterial infections can progress into serious conditions that require treatment.⁵⁶ Thus, advances in technologies which allow us to systematically study the bacterial infections are required to accelerate the development of new therapeutic strategies. Our platform is versatile and suitable for the testing of various microorganisms because the driving force, a hydrodynamic force, acts on any microorganisms in the same manner. We took advantage of our platform's versatility and patterned three distinct bacteria species including clinically relevant *S. aureus*

(Fig. S5†). Also, we demonstrate the examination of interactions between neutrophils and *S. aureus* patterns (Fig. S6 and Movie S4†).

Conclusions

Our system represents a new tool for patterning microorganisms with high precision, in large-scale arrays. Various fungi and bacteria can be patterned in porous microwells, under the effect of hydrodynamic forces. The system can be used to study the growth of microorganisms, the effect of antimicrobials, and the interactions between pathogens and immune cells.

Conflicts of interest

There are no conflicts to declare.

Acknowledgements

This work is funded in part by the National Institutes of Health (GM092804 and DE024468), Shriners Hospital for Children, and the Singapore-MIT Alliance for Research and Technology (SMART). Jae Jung Kim is the recipient of a Samsung Scholarship. We thank Dr. Berent Aldikacti of the BioMEMS Resource Center, Massachusetts General Hospital for the help on confocal microscope imaging.

References

- H. M. P. Consortium, *Nature*, 2012, **486**, 207–214.
- C. A. Lozupone, J. I. Stombaugh, J. I. Gordon, J. K. Jansson and R. Knight, *Nature*, 2012, **489**, 220–230.
- E. A. Grice and J. A. Segre, *Nat. Rev. Microbiol.*, 2011, **9**, 244–253.
- J. He, Y. Li, Y. Cao, J. Xue and X. Zhou, *Folia Microbiol.*, 2015, **60**, 69–80.
- I. Sekirov, S. L. Russell, L. C. Antunes and B. B. Finlay, *Physiol. Rev.*, 2010, **90**, 859–904.
- J. A. Sanford and R. L. Gallo, *Semin. Immunol.*, 2013, **25**, 370–377.
- S. Höfs, S. Mogavero and B. Hube, *J. Microbiol.*, 2016, **54**, 149–169.
- A. Y. Peleg, D. A. Hogan and E. Mylonakis, *Nat. Rev. Microbiol.*, 2010, **8**, 340–349.
- G. Ramage, S. N. Robertson and C. Williams, *Int. J. Antimicrob. Agents*, 2014, **43**, 114–120.
- C. J. Nobile and A. D. Johnson, *Annu. Rev. Microbiol.*, 2015, **69**, 71–92.
- J. D. Bryers, *Biotechnol. Bioeng.*, 2008, **100**, 1–18.
- N. K. Archer, M. J. Mazaitis, J. W. Costerton, J. G. Leid, M. E. Powers and M. E. Shirtliff, *Virulence*, 2011, **2**, 445–459.
- M. Palacios-Cuesta, A. L. Cortajarena, O. Garcia and J. Rodriguez-Hernandez, *Polym. Chem.*, 2015, **6**, 2677–2684.
- A. Cerf, J. C. Cau and C. Vieu, *Colloids Surf., B*, 2008, **65**, 285–291.
- C. M. Costello, J. U. Kreft, C. M. Thomas, D. M. Hammes, P. Bao, S. D. Evans and P. M. Mendes, *Soft Matter*, 2012, **8**, 9147–9155.
- R. R. Hansen, J. P. Hinestrosa, K. R. Shubert, J. L. Morrell-Falvey, D. A. Pelletier, J. M. Messman, S. M. Kilbey, B. S. Lokitz and S. T. Retterer, *Biomacromolecules*, 2013, **14**, 3742–3748.
- C. M. Timm, R. R. Hansen, M. J. Doktycz, S. T. Retterer and D. A. Pelletier, *Biomicrofluidics*, 2015, **9**, 064103.
- N. R. Thirumalapura, A. Ramachandran, R. J. Morton and J. R. Malayer, *J. Immunol. Methods*, 2006, **309**, 48–54.
- J. Choi, J. Yoo, M. Lee, E. G. Kim, J. S. Lee, S. Lee, S. Joo, S. H. Song, E. C. Kim, J. C. Lee, H. C. Kim, Y. G. Jung and S. Kwon, *Sci. Transl. Med.*, 2014, **6**, 267ra174.
- R. Mohan, C. Sanpitakseree, A. V. Desai, S. E. Sevgen, C. M. Schroeder and P. J. A. Kenis, *RSC Adv.*, 2015, **5**, 35211–35223.
- Q. C. Zhang, G. Lambert, D. Liao, H. Kim, K. Robin, C. K. Tung, N. Pourmand and R. H. Austin, *Science*, 2011, **333**, 1764–1767.
- Y. Kuang, I. Biran and D. R. Walt, *Anal. Chem.*, 2004, **76**, 2902–2909.
- I. Biran and D. R. Walt, *Anal. Chem.*, 2002, **74**, 3046–3054.
- C. J. Ingham, A. Sprenkels, J. Bomer, D. Molenaar, A. van den Berg, J. E. T. V. Vlieg and W. M. de Vos, *Proc. Natl. Acad. Sci. U. S. A.*, 2007, **104**, 18217–18222.
- I. Biran, D. M. Rissin, E. Z. Ron and D. R. Walt, *Anal. Biochem.*, 2003, **315**, 106–113.
- C. N. Jones, L. Dimisko, K. Forrest, K. Judice, M. C. Poznansky, J. F. Markmann, J. M. Vyas and D. Irimia, *J. Infect. Dis.*, 2016, **213**, 465–475.
- S. J. Sorensen, M. Bailey, L. H. Hansen, N. Kroer and S. Wuertz, *Nat. Rev. Microbiol.*, 2005, **3**, 700–710.
- J. Q. Boedicker, M. E. Vincent and R. F. Ismagilov, *Angew. Chem., Int. Ed.*, 2009, **48**, 5908–5911.
- B. A. Hense, C. Kuttler, J. Mueller, M. Rothballe, A. Hartmann and J. U. Kreft, *Nat. Rev. Microbiol.*, 2007, **5**, 230–239.
- A. Srinivasan, P. Uppuluri, J. Lopez-Ribot and A. K. Ramasubramanian, *PLoS One*, 2011, **6**, e19036.
- A. Srinivasan, K. P. Leung, J. L. Lopez-Ribot and A. K. Ramasubramanian, *mBio*, 2013, **4**, 00331–13.
- A. Srinivasan, N. S. Torres, K. P. Leung, J. L. Lopez-Ribot and A. K. Ramasubramanian, *mSphere*, 2017, **2**, e00247–17.
- J. R. Rettig and A. Folch, *Anal. Chem.*, 2005, **77**, 5628–5634.
- M. C. Park, J. Y. Hur, K. W. Kwon, S. H. Park and K. Y. Suh, *Lab Chip*, 2006, **6**, 988–994.
- D. Tahk, S. M. Paik, J. Lim, S. Bang, S. Oh, H. Ryu and N. L. Jeon, *Lab Chip*, 2017, **17**, 1817–1825.
- Y. S. Torisawa, B. Mosadegh, S. P. Cavnar, M. Ho and S. Takayama, *Tissue Eng., Part C*, 2011, **17**, 61–67.
- T. Xu, S. Petridou, E. H. Lee, E. A. Roth, N. R. Vyavahare, J. J. Hickman and T. Boland, *Biotechnol. Bioeng.*, 2004, **85**, 29–33.
- J. J. Kim, K. W. Bong, E. Reategui, D. Irimia and P. S. Doyle, *Nat. Mater.*, 2017, **16**, 139–146.
- R. Li, X. Lv, M. Hasan, J. Xu, Y. Xu, X. Zhang, K. Qin, J. Wang, D. Zhou and Y. Deng, *J. Chromatogr. Sci.*, 2016, **54**, 523–530.
- G. D. Brown, D. W. Denning, N. A. Gow, S. M. Levitz, M. G. Netea and T. C. White, *Sci. Transl. Med.*, 2012, **4**, 165rv113.

- 41 H. Tournu and P. Van Dijck, *Int J Microbiol*, 2012, **2012**, 845352.
- 42 M. B. Lohse, M. Gulati, A. Valle Arevalo, A. Fishburn, A. D. Johnson and C. J. Nobile, *Antimicrob. Agents Chemother.*, 2017, **61**, e02749-16.
- 43 J. Chandra and P. K. Mukherjee, *Microbiol. Spectrum*, 2015, **3**, MB-0020.
- 44 R. T. Wheeler, D. Kombe, S. D. Agarwala and G. R. Fink, *PLoS Pathog.*, 2008, **4**, e1000227.
- 45 A. Hopke, N. Nicke, E. E. Hidu, G. Degani, L. Popolo and R. T. Wheeler, *PLoS Pathog.*, 2016, **12**, e1005644.
- 46 L. G. Ng, J. S. Qin, B. Roediger, Y. L. Wang, R. Jain, L. L. Cavanagh, A. L. Smith, C. A. Jones, M. de Veer, M. A. Grimbaldeston, E. N. Meeusen and W. Weninger, *J. Invest. Dermatol.*, 2011, **131**, 2058–2068.
- 47 T. Lammermann, P. V. Afonso, B. R. Angermann, J. M. Wang, W. Kastenmuller, C. A. Parent and R. N. Germain, *Nature*, 2013, **498**, 371–375.
- 48 D. Kreisel, R. G. Nava, W. J. Li, B. H. Zinselmeyer, B. M. Wang, J. M. Lai, R. Pless, A. E. Gelman, A. S. Krupnick and M. J. Miller, *Proc. Natl. Acad. Sci. U. S. A.*, 2010, **107**, 18073–18078.
- 49 C. N. Jones, A. N. Hoang, J. M. Martel, L. Dimisko, A. Mikkola, Y. Inoue, N. Kuriyama, M. Yamada, B. Hamza, M. Kaneki, H. S. Warren, D. E. Brown and D. Irimia, *J. Leukocyte Biol.*, 2016, **100**, 241–247.
- 50 L. Boneschansker, J. Yan, E. Wong, D. M. Briscoe and D. Irimia, *Nat. Commun.*, 2014, **5**, 4787.
- 51 H. Kress, J. G. Park, C. O. Mejean, J. D. Forster, J. Park, S. S. Walse, Y. Zhang, D. Q. Wu, O. D. Weiner, T. M. Fahmy and E. R. Dufresne, *Nat. Methods*, 2009, **6**, 905–909.
- 52 F. Lin, C. M. C. Nguyen, S. J. Wang, W. Saadi, S. P. Gross and N. L. Jeon, *Ann. Biomed. Eng.*, 2005, **33**, 475–482.
- 53 B. Hamza and D. Irimia, *Lab Chip*, 2015, **15**, 2625–2633.
- 54 E. Reátegui, F. Jalali, A. H. Khankhel, E. Wong, H. Cho, J. Lee, C. H. Serhan, J. Dalli, H. Elliott and D. Irimia, *Nat. Biomed. Eng.*, 2017, **1**, 0094.
- 55 K. Kienle and T. Lämmermann, *Immunol. Rev.*, 2016, **273**, 76–93.
- 56 J. J. Weems Jr., *Postgrad. Med.*, 2001, **110**, 24–26, 29–31, 35–26.